

# Mode Spectroscopy and Level Coupling in Ballistic Electron Waveguides

G. Salis, T. Heinzel, and K. Ensslin

*Solid State Physics Laboratory, ETH Zürich, 8093 Zürich, Switzerland*

O. J. Homan and W. Bächtold

*Institut für Feldtheorie und Höchstfrequenztechnik, ETH Zürich, 8092 Zürich, Switzerland*

K. Maranowski and A. C. Gossard

*Materials Department, University of California, Santa Barbara, Ca 93106, USA*

(September 5, 2018)

A tunable quantum point contact with modes occupied in both transverse directions is studied by magnetotransport experiments. We use conductance quantization of the one-dimensional subbands as a tool to determine the mode spectrum. A magnetic field applied along the direction of the current flow couples the modes. This can be described by an extension of the Darwin-Fock model. Anticrossings are observed as a function of the magnetic field, but not for zero field or perpendicular field directions, indicating coupling of the subbands due to nonparabolicity in the electrical confinement.

PACS numbers: 73.23.Ad, 73.20.Dx

Conductance quantization in quasi one-dimensional (1D) systems [1,2] is one of the crucial discoveries in the physics of semiconductor nanostructures [3]. Usually, such 1D channels (quantum point contacts - QPCs) are realized by split gate electrodes fabricated on Ga[Al]As heterostructures. In analogy to optical waveguides [4], QPCs are also known as “ballistic electron waveguides”. Meanwhile, QPCs have become a key device for transport experiments in low-dimensional systems [3]. Typically, they are realized in an extreme limit where the confinement of the two-dimensional electron gas at the heterointerface is so strong that only the lowest two-dimensional (2D) subband lies below the Fermi energy. The mode spectrum of a QPC defined in such a heterostructure is dominated by the lateral confinement which can be tuned by appropriate voltages on the split gate electrodes. The modes, characterized by a single quantum number, are well separated in energy and do not couple to each other.

Here, we present experimental results from a ballistic electron waveguide realized by a split gate electrode on top of a wide electron system in a parabolic quantum well. The 1D energy levels can be described by two quantum numbers for the two confining directions. A rich mode spectrum as a function of gate voltages and magnetic fields, applied in different directions with respect to the electron waveguide, is observed. While all levels move upwards in energy when a magnetic field is applied in the plane of the quantum well but perpendicular to the waveguide, one finds also levels moving downwards in energy as a function of a parallel magnetic field. The confining potential landscape inside the constriction can be studied by analyzing these measurements. We explain our data in terms of a generalization of the Darwin-Fock model, which describes the energy spectrum of a circular disc in magnetic fields perpendicular to it [5]. Thus, our

experiment is closely related to those on quantum dots [6].

Level crossings and anticrossings are observed, manifesting themselves as suppressed conductance plateaus. We find that non-parabolicity in the confining potential induces anticrossings as a function of the parallel field. Furthermore, the mode crossings give an absolute measure for the energy spectrum, independent of the lever arms with respect to gate voltages.

The parabolic quantum well consists of a 76 nm wide  $\text{Al}_x\text{Ga}_{1-x}\text{As}$  layer, where the averaged Al content  $x$  has been varied parabolically during molecular beam epitaxy [7]. In the center of the well, three monolayers of  $\text{Al}_{0.05}\text{Ga}_{0.95}\text{As}$  have been grown, serving as a probe for the position of the wave function in the well [8,9]. A  $n^+$  doped layer, used as a back gate electrode, has been integrated 1.35  $\mu\text{m}$  below the well and contacted independently. A 50  $\mu\text{m}$  wide Hall bar structure has been defined by wet chemical etching, and the electron gas is accessed via Ni-AuGe Ohmic contacts. The split gate has been fabricated by electron beam lithography, and defines a nominally 400 nm wide and 300 nm long channel. The parabolic potential along the growth direction  $z$  defines the waveguide in one dimension. The other confining direction ( $y$ ) is constricted by applying appropriate voltages  $U_{\text{sg}}$  to the split-gate electrode with respect to the electron gas. The back gate can be used to change the electron density and thus the constriction width. With  $U_{\text{sg}}$ , one tunes the difference between the Fermi energy  $E_F$  and the conduction band edge and thus the number of occupied 1D subbands.

The measurements have been performed in the mixing chamber of a  $^3\text{He}/^4\text{He}$  dilution refrigerator with a base temperature of 60 mK; we estimate the electron temperature to be about 100 mK. At zero back-gate voltage

$U_{\text{bg}}$ , two subbands are occupied with sheet densities of  $n_1 = 2.6 \times 10^{15} \text{ m}^{-2}$  and  $n_2 = 2.0 \times 10^{15} \text{ m}^{-2}$ . A series resistance of about  $450 \Omega$  due to the leads between the voltage probes and the QPC is subtracted.

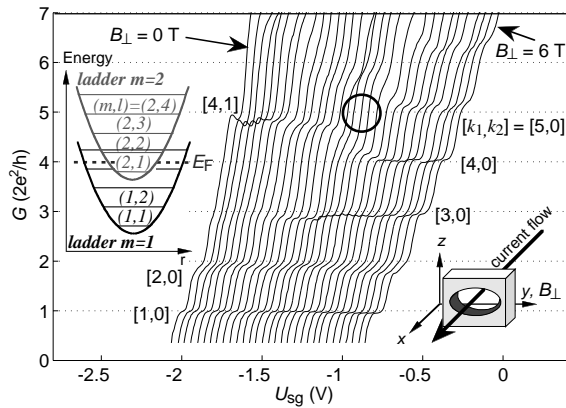


FIG. 1. Measured conductance  $G$  of the electron waveguide, sketched in the right inset, as a function of  $U_{\text{sg}}$  ( $U_{\text{bg}} = 0$ ) and for different  $B_{\perp}$ , varying between 0 and 6 T in steps of 0.2 T. Subsequent curves are horizontally offset for clarity by 40 mV. The subbands are labelled by  $(m, l)$ , and the number of occupied subbands is denoted by  $[k_1, k_2]$  as explained in the text. Some plateaus can be suppressed and recovered by  $B_{\perp}$ . Left inset: scheme of the two subband ladders, plotted vs. spatial coordinate  $r$ . In this example,  $[k_1, k_2] = [4, 1]$  is shown. The circle in the main figure denotes a situation where the  $(1, 4)$  - level is degenerate with the  $(2, 1)$  - level.

We have investigated the electron waveguide in magnetic fields up to 6 T, in directions parallel ( $B_{\parallel}$ ) and perpendicular ( $B_{\perp}$ ) to the flow of current through the QPC (but always in the plane defined by the quantum well). Figure 1 shows the measured conductance  $G$  as a function of  $U_{\text{sg}}$  for a set of  $B_{\perp}$  between 0 and 6 T. conductance plateaus, quantized in units of  $2Ne^2/h$ , with  $N$  being an integer, are visible up to  $N = 6$ . While the lowest two plateaus are only slightly modified by  $B_{\perp}$ , the higher plateaus vanish for certain ranges of  $B_{\perp}$ . The circle in Fig. 1 marks a regime in which the  $N = 5$  plateau is suppressed. Similar suppressions are observed when  $B_{\parallel}$  or  $U_{\text{bg}}$  is varied (not shown).

The energy levels of our electron waveguide are labelled by two quantum numbers  $l$  and  $m$ , belonging to the two confinement directions in  $y$ - and  $z$ -directions, respectively. A ladder of 1D states is attributed to each of the two occupied 2D subbands. Our system can thus be seen as being composed of 2 coupled QPCs in parallel [10]. In this respect, it is similar to two separated QPCs arranged in parallel, as investigated in Refs. [11–14]. However, the 1D ladders in our sample reside in identical host potentials and have large wave function overlaps. We label these states by  $(m, l)$ , where  $m = \{1, 2\}$  denotes the ladder to which the state belongs, and  $l$  labels the states inside ladder  $m$ . Furthermore, the number of occupied

subbands attributed to ladder  $m$  is denoted by  $k_m$ . The total number  $N$  of 1D levels below the Fermi energy  $E_F$  is thus given by  $N = k_1 + k_2$ . The suppression of the plateau at  $N = 5$ , for example, can be understood as a degeneracy of the levels  $(1, 4)$  and  $(2, 1)$ . If such two degenerated levels cross the Fermi energy, the conductance changes by  $4e^2/h$ . Therefore, no plateau at  $N = 5$  is observable in this example.

The energy spectrum and its dependence on magnetic field can be visualized by plotting the transconductance  $dG/dU_{\text{sg}}$  with respect to  $U_{\text{sg}}$  and magnetic field [Fig. 2(a) and (b)].

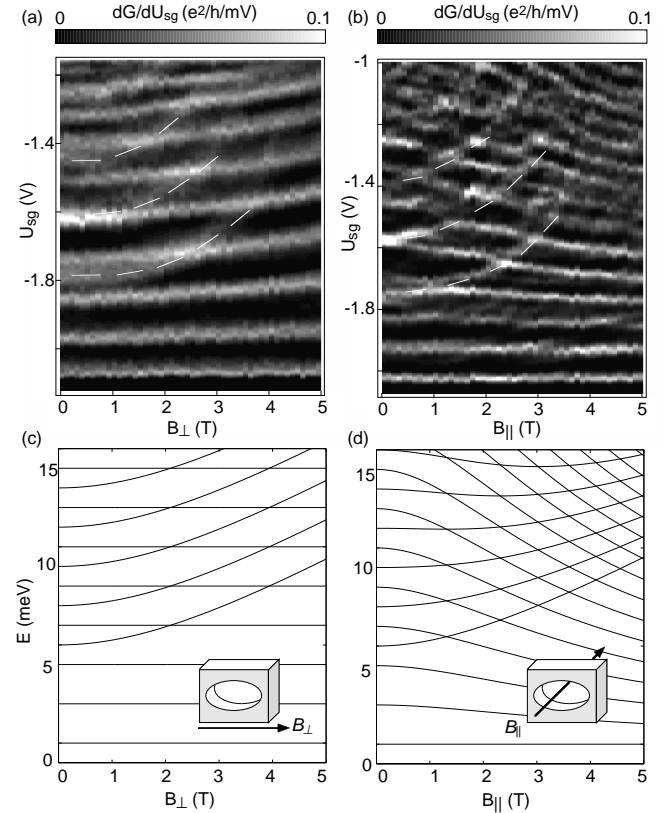


FIG. 2. Grayscale plot of  $dG/dU_{\text{sg}}$  as a function of  $U_{\text{sg}}$  and  $B_{\perp}$  (a), and  $B_{\parallel}$ , respectively (b). A high transconductance is related to a crossing between  $E_F$  and a 1D subband level. The dashed lines are guides to the eye. In (c) and (d), calculated energy levels for a parabolically confined waveguide with  $\omega_y = 2 \text{ meV}$  and  $\omega_z = 5 \text{ meV}$  are shown.

On a plateau in  $G(U_{\text{sg}})$ ,  $E_F$  lies between two 1D levels. This corresponds to a low transconductance (dark regions). On the other hand, on a transconductance peak a 1D level crosses  $E_F$  (bright regions). With increasing  $U_{\text{sg}}$ , the subband ladders move upwards with respect to  $E_F$  and thus the mode spectrum can be scanned. The bright lines in Fig. 2 reflect the 1D levels plotted vs.  $B$ . In both cases, two ladders of 1D subbands are observed whose

magnetic field behavior depends on both the ladder index  $m$  as well as on the direction of the magnetic field. In perpendicular fields, nine levels of ladder 1 are visible, showing a weak shift towards higher energies in increasing magnetic fields, while the energy separation between subsequent levels increases. The four visible modes belonging to the second ladder show a much stronger upwards shift in energy with increasing magnetic field. In parallel magnetic fields, the mode spectrum shows two striking differences. First of all, the states belonging to ladder 1 shift downwards in energy for  $B_{\parallel} > 1$  T, while the states of the second ladder are essentially insensitive to the direction of the magnetic field. Second, anticrossings form between  $m = 1$  - states and  $m = 2$  - states (Fig. 3).

By varying  $U_{\text{sg}}$ , not only the subband ladders are displaced with respect to  $E_F$ , but also the step-size of the ladders changes due to the modification of the waveguide shape. In addition, the lever arm  $\alpha = dE/dU_{\text{sg}}$  may not be perfectly constant. Therefore,  $U_{\text{sg}}$  can only be a coarse measure for the energy. We can estimate  $\alpha$  by measuring the smearing-out of a conductance plateau as a function of the source-drain voltage [15], and find an average subband-spacing of 2 meV at  $B = 0$ , which has to be compared with a step width in  $U_{\text{sg}}$ . We obtain  $\alpha \approx 0.02 \text{ meV/mV}$ . However, the energy scale is fixed by the crossing points of mode levels. In the following, we compare the measured mode spectrum with a calculation of the energy levels of a 2D constriction in a magnetic field. For the  $B_{\perp}$ -case [Figs. 2(a) and (c)], the magnetic field along the  $y$ -direction modifies the dispersion relation in  $x$ -direction and thus the effective mass, whereas the  $z$ -confinement is enhanced due to the diamagnetic term proportional to  $B_{\perp}^2$ . A coupling term of the  $z$ - and  $x$ -direction results in a shift of the Fermi surface in  $k_x$ -direction. Neglecting electron-electron interactions, no coupling of the  $y$ - and  $z$  direction is expected for a separable confinement potential  $V(y, z)$ . For a parabolic confinement  $V(y, z) = m^*(\omega_y^2 y^2 + \omega_z^2 z^2)/2$  the subband energies are given by  $E_{ml} = \hbar\omega_1(l - \frac{1}{2}) + \hbar\sqrt{\omega_z^2 + \omega_{\perp}^2}(m - \frac{1}{2})$ , where  $\omega_{\perp}$  is the cyclotron frequency  $eB_{\perp}/m^*$  [16]. Figure 2(c) shows the energy fan for  $\omega_y = 2$  meV and  $\omega_z = 5$  meV. The levels cross each other at identical magnetic fields and without level repulsions. The measured spread of the step size with increasing  $B_{\perp}$  [Fig. 2(a)] can be explained by a field-dependent reduction of the density of states in the 2DEG, due to the modified dispersion relation, leading to a decrease of  $E_F$  relative to the conduction band bottom with increasing  $B_{\perp}$  [17,18].

$B_{\parallel}$  couples the two confining directions  $y$  and  $z$ . If a parabolic confinement with rotational symmetry is assumed, this leads to the ordinary Zeeman effect, described by the Darwin-Fock states [5]. Within this model, the eigenstates of a circular disc (or a wire with a circular cross section, respectively) with different angular

momenta are degenerate at  $B_{\parallel} = 0$ . This degeneracy is lifted by non-zero  $B_{\parallel}$ , and, depending on its angular momentum, the energy of one level can either increase or decrease. For a non-circular confinement potential as realized in our QPC, the degeneracy is already lifted at  $B = 0$ .

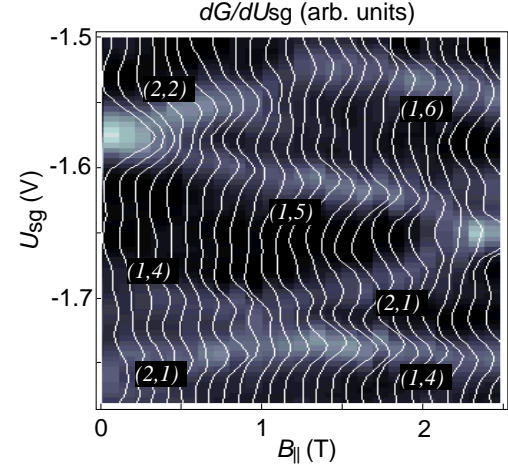


FIG. 3. Close-up of Fig. 2(b) showing anticrossing of the  $(2, 1)$  - level with the  $(1, 4)$  - level. In addition to the grayscale, the individual transconductance traces are shown.

A calculation for parabolic confinements with arbitrary  $\omega_y$  and  $\omega_z$  gives the result [19]

$$E_{ml} = \hbar\omega_1(l - \frac{1}{2}) + \hbar\omega_2(m - \frac{1}{2}), \quad (1)$$

with

$$\omega_{1,2}^2 = \frac{1}{2}(\omega_{\parallel}^2 + \omega_y^2 + \omega_z^2) \pm \sqrt{\left(\omega_{\parallel}^2 + \omega_y^2 + \omega_z^2\right)^2 - \omega_y^2\omega_z^2}. \quad (2)$$

Here we used  $\omega_{\parallel} = eB_{\parallel}/m^*$ . The larger of the two frequencies  $\omega_1$  and  $\omega_2$  increases with  $B_{\parallel}$ , while the smaller one decreases. Figure 2(d) shows a calculation for  $\omega_y = 2$  meV and  $\omega_z = 5$  meV, which reproduces the observed decrease of the 1D subband levels of Fig. 2(b). There are two qualitative differences between the simple model of Eq. 1 and the measurements: First, the levels do not cross at the same  $B_{\parallel}$  as in the model, and second the measured levels show anticrossings. The anticrossing is particularly pronounced between, for example,  $(1, 4)$  and  $(2, 1)$ , while it is much weaker for other levels, like  $(1, 5)$  and  $(2, 1)$  (Fig. 3).

As seen in Fig. 2(a), no anticrossing is observed for  $B_{\perp}$ . Similarly, the traces of transconductance maxima cross regularly as a function of  $U_{\text{bg}}$  for  $B = 0$ . This indicates that the electric confinement potential is separable in  $y$  and  $z$ -directions. However, for finite fields  $B_{\parallel}$ , the magnetic confinement prevents a decoupling of the Hamiltonian into two independent oscillators if the QPC

confinement is not exactly parabolic, leading to level anticrossings. We therefore argue that the observed anticrossings have their origin in nonparabolicities of the confining potential. For square well electric confinements, a complicated level structure with unregular anticrossings was calculated [20,21]. In our samples, the dominant non-parabolicity may come from electron-screening, giving rise to a more rectangularly shaped effective potential in  $z$ -direction. We have calculated the influence of the three monolayers wide potential perturbation in the center of the quantum well, and obtain anticrossings in first-order perturbation theory, which are too small to account for the observed effects.

No clear signature of level locking could be observed, although predicted for coupled one-dimensional wires [22].

For the Darwin-Fock model, it is irrelevant whether the waveguide extends to infinity in the direction parallel to the magnetic field, the system is a truly 2D disc. Quantum dots are usually described as such 2D discs and have not only been thoroughly studied theoretically, but also widely investigated by magnetotransport measurements [6]. In those experiments, the dot is weakly coupled to two leads via tunnel barriers. Such small quantum dots with sizes comparable to the cross section of our waveguide are highly interesting also from a theoretical point of view, since interaction effects, in particular Coulomb blockade as well as exchange and correlation corrections, and their influence on the energy spectrum for small occupation numbers can be experimentally determined. However, it is difficult to distinguish between effects originating from the shape of the confining potential and those from interaction effects. In that sense, our QPC provides a perfect reference system, since by effectively extending the dot to infinity in the direction of the magnetic field, interaction effects are essentially turned off. As can be seen from the above measurements, the magnetic field dependence of the energy levels is nontrivial even in the absence of interactions.

In conclusion, we have experimentally investigated the 1D subband energies of a ballistic electron waveguide realized in a semiconductor parabolic quantum well by measuring its transconductance as a function of gate voltage and magnetic fields, aplied in different directions. Depending on their mode index, energy levels may shift upwards or downwards in energy under parallel magnetic fields, while they always shift to higher energies in perpendicular magnetic fields. We have modelled this behavior in terms of an analytical model. In the case where  $B$  is oriented perpendicular to the axis of the QPC, coupling between one-dimensional subbands is neither observed nor expected. For field directions along the axis, a coupling, manifested as level anticrossings, is observed and interpreted as a consequence of nonparabolic confinement.

We acknowledge valuable discussions with A. Lorke and J. P. Kotthaus. This project was financially sup-

ported by the Swiss Science Foundation, AFOSR grant F 49620-94-1-0158 and the NSF Center for Quantized Electronic Structures (QUEST).

---

[1] B. J. van Wees, H. van Houten, C. W. J. Beenakker, J. G. Williamson, L. P. Kouwenhoven, D. van der Marel, and C. T. Foxon, *Phys. Rev. Lett.* **60**, 848 (1988).

[2] D. A. Wharam, T. J. Thornton, R. Newbury, M. Pepper, H. Ahmed, J. E. F. Frost, D. G. Hasko, D. C. Peacock, D. A. Ritchie, and G. A. C. Jones, *J. Phys. C* **21**, L209 (1988).

[3] for a review, see H. van Houten, C.W. J. Beenakker, and B.J. van Wees, *Quantum Point Contacts*, in *Semicond. and Semimet.* **35**, ch. 2 (1992).

[4] A. Yariv, *Quantum Electronics* 3rd ed., Wiley, New York 1989.

[5] C. G. Darwin, *Proc. Cambridge Philos. Soc.* **27**, 86 (1931); V. Fock, *Z. Phys.* **47**, 446 (1928).

[6] for a review, see L.P. Kouwenhoven, C.M. Marcus, P.L. McEuen, S. Tarucha, R.M. Westervelt, and N.S. Wingreen, pp. 2-110, in *Mesoscopic Electron Transport*, Kluwer 1997.

[7] A. C. Gossard, *IEEE J. Quant. Electron.* **22**, 1649 (1986).

[8] G. Salis, B. Graf, K. Ensslin, K. Campman, K. Maranowski, and A. C. Gossard, *Phys. Rev. Lett.* **79**, 5106 (1997).

[9] G. Salis, P. Wirth, T. Ihn, T. Heinzel, K. Ensslin, K. Campman, K. Maranowski, and A. C. Gossard, to appear in *Phys. Rev. B* **59**, (1999).

[10] G. Salis, T. Heinzel, K. Ensslin, O.J. Homan, W. Bächtold, K. Maranowski, and A.C. Gossard, *Proceedings of the 23rd International Conference on the Physics of Semiconductors*, in print.

[11] C. G. Smith, M. Pepper, R. Newbury, H. Ahmed, D. G. Hasko, D. C. Peacock, J. E. F. Frost, D. A. Ritchie, G. A. C. Jones, and G. Hills, *J. Phys.: Condens. Matter* **1**, 6763 (1989).

[12] P. J. Simpson, D. R. Mace, C. J. B. Ford, I. Zailer, M. Pepper, D. A. Ritchie, J. E. F. Frost, M. P. Grimshaw, and G. A. C. Jones, *Appl. Phys. Lett.* **63**, 3191 (1993).

[13] I. M. Castleton, A. G. Davies, A. R. Hamilton, J. E. F. Frost, M. Y. Simmons, D. A. Ritchie, and M. Pepper, *Physica B* **251**, 157 (1998).

[14] K.J. Thomas, M. Y. Simmons, W.R. Tribe, A. G. Davies, and M. Pepper, *cond-mat/9901161* (1999).

[15] L. P. Kouwenhoven, B. J. Wees, C. J. P. M. Harmans, J. G. Williamson, H. van Houten, C. W. J. Beenakker, C. T. Foxon, and J. J. Harris, *Phys. Rev. B* **39**, 8040 (1989).

[16] A. G. Scherbakov, E. N. Bogachev and U. Landman, *Phys. Rev. B* **53**, 4054 (1996).

[17] F. Stern, *Phys. Rev. Lett.* **21**, 1687 (1968).

[18] G. Salis, B. Ruhstaller, K. Ensslin, K. Campman, K. Maranowski, and A. C. Gossard, *Phys. Rev. B* **58**, 1436 (1998).

[19] B. Schuh, *J. Phys. A* **18**, 803 (1985).

- [20] W. Hansen, T. P. Smith III, K. Y. Lee, J. A. Brum, C. M. Knoedler, J. M. Hong, and D. P. Kern, Phys. Rev. Lett. **62**, 2168 (1989).
- [21] M. Robnik, J. Phys. A **19**, 3619 (1984).
- [22] Y. Sun and G. Kirczenow, Phys. Rev. Lett. **72**, 2450 (1994).